Supporting Information

Ferrer *et al.* 10.1073/pnas.0706124105

SI Text

α-Actinin Immobilized Directly on Surface. To immobilize α-actinin directly on surface, we introduced 100 nM α-actinin in 1× F-buffer with 2 mg/ml BSA and incubated it for 30 min. After washing the sample with 200 μl of 1× F-buffer, we added 20 μl of biotinylated actin incubated previously with streptavidin-coated beads. After 30 min of incubation, we washed the sample with 200 μl of 1× F-buffer and sealed the flow cell with nail polish. The procedure for rupturing the bond was the same as described in *Materials and Methods*.

The rupture-force distribution is depicted in Fig. S2. The loading rate was ≈5 pN/s, and the most probable rupture force was 6.99 ± 4.40 pN. The forces recorded for this immobilization scheme are considerably lower than those measured with the native-like assay, demonstrating that assay design must be considered an important factor when interpreting the results. An alternative method for surface binding performed by Miyata *et al.* (1) used nitrocellulose-coated glass to immobilize α-actinin. Unbinding forces in this assay were measured to range from 1.4–44 pN with an average magnitude of 18 pN, similar to rupture forces measured in our system.

Direct Unfolding Measurements of Filamin. To directly measure the force to unfold filamin, we prepared biotin-labeled filamin using biotin-linked *N*-succinimide ester (Sigma) linkage to random filamin cysteines using a 10:1 ratio for labeling filamin according to the manufacturer's recommended protocol. The biotin-labeled filamin molecules were diluted in 1 mg/ml BSA and introduced to clean etched coverslip surfaces to achieve non-specific binding of the filamin to glass. After 20 min of incubation, the flow cell was washed with 1 mg/ml BSA, and then 800-nm diameter streptavidin-coated beads were introduced in the presence of 3 mg/ml BSA. Tethered beads were centered and pulled as described in *Materials and Methods*. Stage velocity was 0.08 μm/s. We note that due to the random nature of biotin labeling and surface attachment of the filamin molecule, the tether length is unknown but is estimated to be less than the 150-nm molecular length. As a result, force on the filamin molecule will be amplified due to a lever arm action from force on the bead, see *Inset* in Fig. S5*b* (2, 3).

Hysteresis Measurements. Hysteresis was observed by using a method similar to that used in the pulling measurements described in *Materials and Methods*, but a force threshold was set to trigger the stage to reverse direction. A second trigger, positioned at a low force threshold, was then activated to reverse the stage to the original direction. Bead-position data were recorded at 3 kHz and averaged with a 25-point window.

High Loading Rate Pulls on the Actin–Filamin–Actin System. We performed a small number of high loading rate experiments on the actin–filamin–actin system, at pulling rates approaching that of the AFM experiment by Furuike *et al.* (4), (stage velocities of 5 μm/s). In the few events we obtained, we noticed an increase in the likelihood of observing unfolding-type transitions. One in particular shows a region consistent with sawtooth-like multiple unfoldings of domains (Fig.S5*a*). We believe the likelihood of unfolding increases at these loading rates, which are comparable with those used in AFM experiments.

Model Implementation. To estimate the parameters describing the molecular interactions of interest, we implemented the theoretical model developed by Hummer and Szabo (5). The rupture-force probability distribution is given by

$$p(F) = \frac{\beta}{\kappa_s \nu}\left[\frac{dS}{dt}\right]_t^* = \frac{(\beta G + \kappa s x_t)}{\kappa_s \nu}, \qquad [1]$$

where $S(t)$ is the survival probability of the system defined as

$$S(t) = \exp\left[-\frac{k_{\text{off}} e^{-\frac{1}{2}\kappa_s (x^\ddagger)^2}}{\kappa_s \nu x^\ddagger (\kappa_m/\kappa)^{\frac{3}{2}}}\left(e^{\kappa_s \nu x^\ddagger t - (\kappa_s \nu t)^2/(2\kappa)} - 1\right)\right], \qquad [2]$$

where κ_s and κ_m are the effective spring constants of the pulling system and the molecular spring, respectively, both divided by k_BT, $\kappa = \kappa_s + \kappa_m$, and ν is the pulling velocity. Note that $\kappa_s \nu/\beta = \dot{F}$ in Eq. **1**. It is important to notice that by scaling with β, the harmonic spring constants κ_s, κ_m, and κ have units of inverse length squared. To simplify the expression of Eq. **2**, we define the following new variables:

$$A = \frac{k_0 e^{-\frac{1}{2}\kappa_s (x^\ddagger)^2}}{\kappa_s \nu x^* (\kappa_m/\kappa)^{\frac{3}{2}}} \qquad [3]$$

$$B = \kappa_s \nu x^\ddagger \qquad [4]$$

$$C = \frac{(\kappa_s \nu)^2}{2\kappa}. \qquad [5]$$

In addition, with a simple algebraic manipulation of the expression for t^*, we get

$$t^* = \frac{\beta F \nu + \kappa_s \nu x^\ddagger}{\kappa_s \nu^2} = \frac{\beta F \nu + B}{\kappa_s \nu^2}. \qquad [6]$$

After taking the time derivative of $S(t)$ and substituting the newly defined variables, the analytical expression for the probability distribution of rupture forces is given by

$$p(F) = \beta \frac{BA - 2AC\left(\frac{\beta F \nu + B}{\kappa_s \nu^2}\right)}{\kappa_s \nu} \cdot \exp\left[\frac{B(\beta F \nu + B)}{\kappa_s \nu^2} - C\left(\frac{\beta F \nu + B}{\kappa_s \nu^2}\right)^2\right] \times \exp\left\{-A\left[\exp\left[\frac{B(\beta F \nu + B)}{\kappa_s \nu^2} - C\left(\frac{\beta F \nu + B}{\kappa_s \nu^2}\right)^2\right] - 1\right]\right\} \qquad [7]$$

The force histograms are fitted to Eq. **7** to obtain values for A, B, and C, and then using Eqs. **3**, **4**, and **5**, we solve for k_0, $x^\ddagger$, and κ_m.

Rupture Location. In the current assay, rupture between the actin/ABP/actin interactions can occur at either end where the ABP binds to actin or between the subunits of the ABP dimer. Although it would be useful to know the exact location of rupture (upper or lower filament in Fig. 1), the focus of this study is to probe the complex as a whole independent of which intera tion is the weakest. We believe that rupture is not likely to occur

between the dimers because in previous AFM force-extension experiments with filamin, the dimerized protein was able to sustain forces >200 pN without rupturing (4). Thus, it is reasonable to assume that the dimer interactions in an ABP are stronger than those between the ABP and actin.

By developing a native-like single-molecule assay, we were able to measure the forces required to rupture the molecular linkage between an ABP and two actin filaments. We found that, at least for the α-actinin/actin interaction, the rupture force required when α-actinin was immobilized directly onto the surface was much lower than the force required for the current assay. It is possible that the binding to two filaments instead of one can lead to a more energetically favored conformational state of α-actinin, enhancing the stability of the interaction. This leads to the speculation that the cell might use this mechanism to further regulate the formation of F-actin structures at specific locations.

Approximation of Maximum Stress in Reconstituted Networks from Single-Molecule Rupture Forces. If we assume an isotropic F-actin network cross-linked by filamin with force distributed between four cross-links with a characteristic size L_c, then the maximum stress that the network can withstand is $\sigma_{max} \approx 4F_{max}/L_c^2$, where F_{max} is the rupture force at each cross-link. Tharmann *et al.* (6) showed that for an isotropic network cross-linked with heavy meromyosin (HMM) in rigor state, $L_c \sim [1]c_c^y(\xi^2 l_p^{0.5})^{0.4}$, where c_c is the concentration of cross-linker, l_p is the persistence length of actin ($\approx$16 μm), and ξ is the mesh size, in micrometers, defined as $\xi = 0.3/c_a^{0.5}$ (7), and c_a is the actin concentration in units of mg/ml. The exponent y was estimated to be -0.4 for HMM, and in the absence of a better approximation, we use the same value of y to estimate L_c for networks with filamin. Using $c_a = 12$ μM, and $c_c = 0.12$ μM [similar to those in Gardel *et al.* (8)], we estimate $\sigma_{max} \approx$12–42 Pa for a rupture force range of 20–70 pN. This $\sigma_{\max}$ compares well with the one measured by Gardel *et al.* of $\approx$60 Pa under similar conditions.

1. Miyata H, Yasuda R, Kinosita K (1996) Strength and lifetime of the bond between actin and skeletal muscle alpha-actinin studied with an optical trapping technique. *BBA-Gen Subjects* 1290:83–88.
2. Chang KC, Hammer DA (1996) Influence of direction and type of applied force on the detachment of macromolecularly-bound particles from surfaces. *Langmuir* 12:2271–2282.
3. Stout AL, Webb WW (1998) Optical force microscopy. *Methods Cell Biol* 55:99–116.
4. Furuike S, Ito T, Yamazaki M (2001) Mechanical unfolding of single filamin A (ABP-280) molecules detected by atomic force microscopy. *FEBS Lett* 498:72–75.
5. Hummer G, Szabo A (2003) Kinetics from nonequilibrium single-molecule pulling experiments. *Biophys J* 85:5–15.
6. Tharmann R, Claessens MMAE, Bausch AR (2007) Viscoelasticity of isotropically cross-linked actin networks. *Phys Rev Lett* 98:088103.
7. Schmidt CF, Barmann M, Isenberg G, Sackmann E (1989) Chain dynamics, mesh size, and diffusive transport in networks of polymerized actin—a quasielastic light-scattering and microfluorescence study. *Macromolecules* 22:3638–3649.
8. Gardel ML, *et al.* (2006) Stress-dependent elasticity of composite actin networks as a model for cell behavior. *Phys Rev Lett* 96:088102.

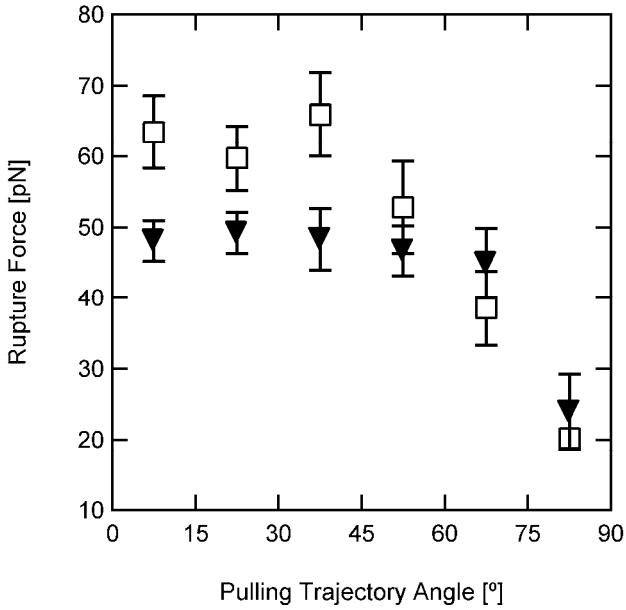

Fig. S1. Rupture force vs. angle between stage direction and displacement of bead for α-actinin/actin (▼) and the filamin/actin interactions (□). Angles were calculated from the pulling trajectory of the bead just before a rupture event. Error bars indicate standard error of the mean.

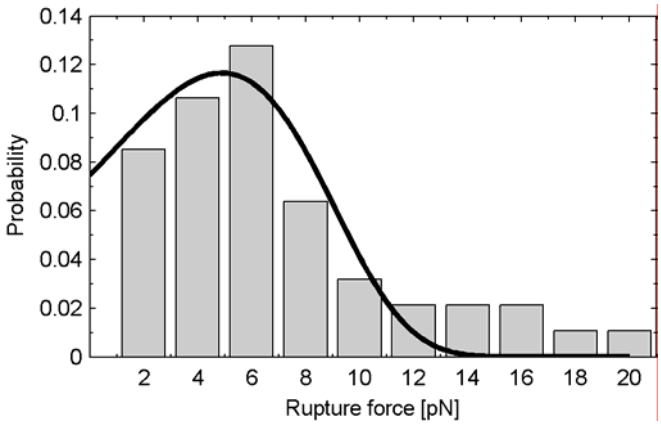

Fig. S2. Rupture-force distribution between α-actinin immobilized on surface and a single actin filament. The loading rate is $\approx$5 pN/s, and the rupture force is 6.99 $\pm$ 4.40 pN.

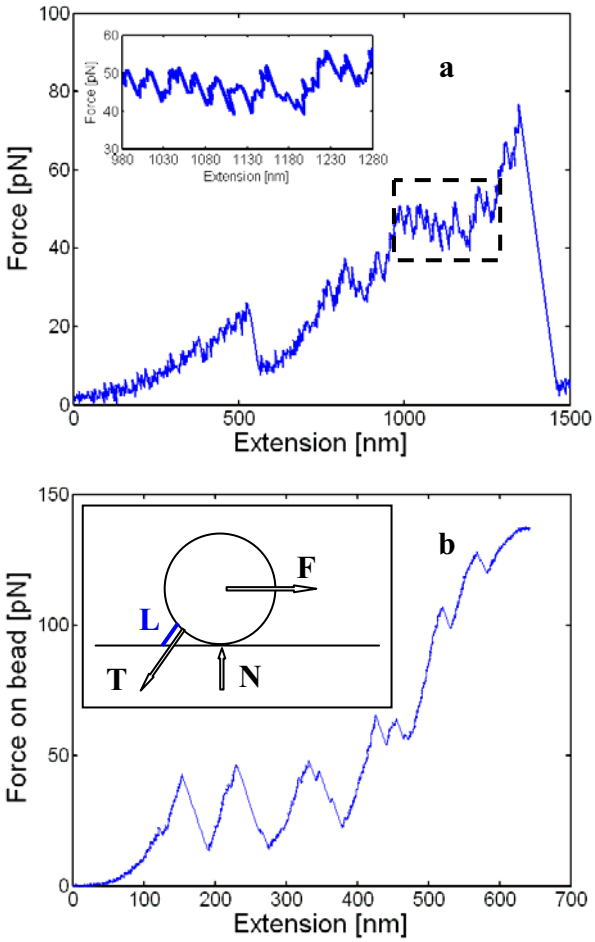

Fig. S3. High loading rates on filamin–actin system, and stretching of a single filamin molecule. (*a*) Force-vs.-extension curve, showing extension and rupture for filamin-actin at high stage velocity, 5 μm/s. The *Inset* is a blowup of the dotted box region exhibiting a flattening of the force-vs.-extension curve and periodic structure, with a spatial period of 30 nm, attributed to unfolding of repeat domains of filamin. (*b*) The event is an example of a force-vs.-extension curve for unfolding filamin directly showing multiple transitions consistent with opening of one or more filamin domains. Note that the bead may be in contact with the surface, necessitating an amplification correction to obtain force on the tether due to interaction with the surface. In the *Inset*, F is the applied force on the bead by optical tweezers, T is the tension on the filamin, N is the normal force by contact with the surface, and L is the length of filamin tether.

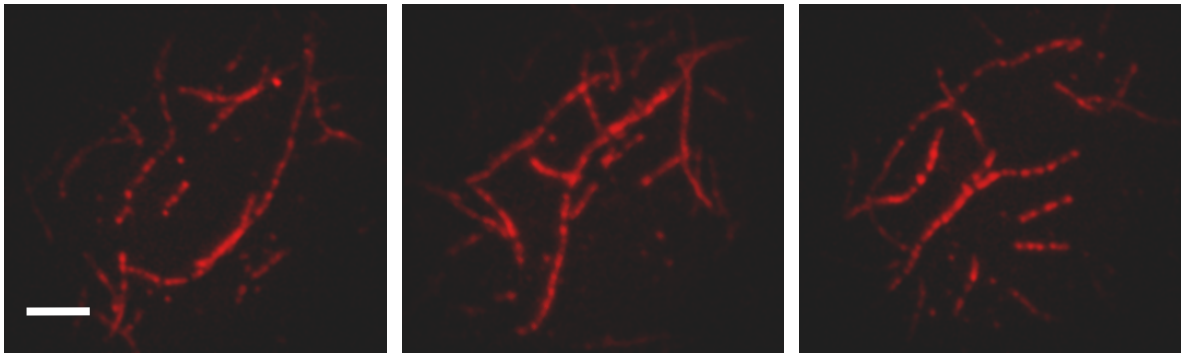

Fig. S4. Additional micrographs showing examples of surface-bound actin filaments labeled with Alexa Fluor 555 phalloidin. The flow cell direction is along the diagonal from the lower left to upper right. (Scale bar: 5 μm.)

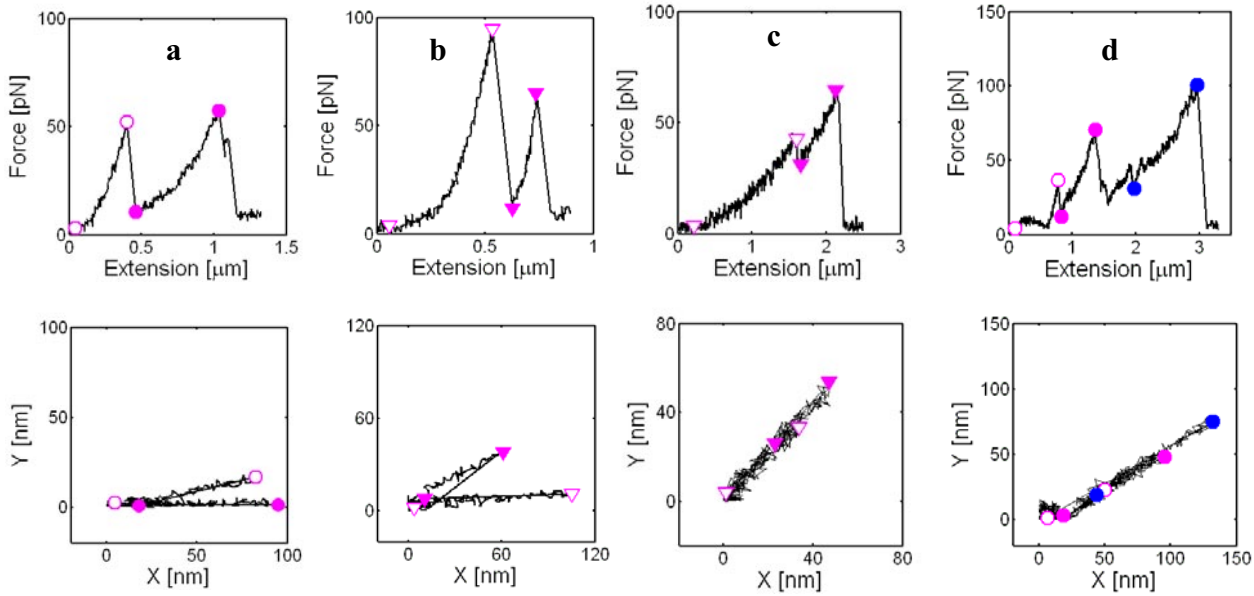

Fig. S5. Rupture of the actin-filamin–actin interaction. (*Upper*) Force-extension curves. (*Lower*) Respective *x*–*y* plots. Columns *a* and *b* show transitions where the force does not relax to baseline, and the pulling trajectory follows a different angle after initial drop in force. Columns *c* and *d* show transitions where the force does not relax to baseline, but the transitions follow the same trajectory.